ELSEVIER

Contents lists available at ScienceDirect

Applied Geochemistry

journal homepage: www.elsevier.com/locate/apgeochem





Isoprene peroxy chemistry operates competitively in areas of East China

Kate DeMarsh ^{a,1}, Hongli Wang ^{b,**,1}, Yaqin Gao ^b, Zeyi Moo ^a, Peizhi Hao ^a, Shengao Jing ^b, Shengrong Lou ^b, Cheng Huang ^b, Song Guo ^c, Sihua Lu ^c, Limin Zeng ^c, Angeles Elias ^a, Siyuan Wang ^{d,e}, Xuan Zhang ^{a,*}

- ^a Department of Life and Environmental Sciences, University of California, Merced, CA, 95343, USA
- b State Environmental Protection Key Laboratory of Formation and Prevention of Urban Air Pollution Complex, Shanghai Academy of Environmental Sciences, Shanghai,
- c State Key Joint Laboratory of Environmental Simulation and Pollution Control, College of Environmental Sciences and Engineering, Peking University, Beijing, 100871, China
- ^d Cooperative Institute for Research in Environmental Sciences, University of Colorado, Boulder, CO, USA
- ^e National Oceanic and Atmospheric Administration (NOAA), Chemical Sciences Laboratory, Boulder, CO, USA

ARTICLE INFO

Editorial Handling by: Zimeng Wang

Keywords: Isoprene Methacrolein Methyl vinyl ketone Nitrogen oxides

ABSTRACT

We validated the recently updated Caltech Isoprene Mechanism (CIM), which represents the complex dynamics of isoprene peroxy isomers through repetitive O₂ addition and dissociation reactions, using a dataset synthesized from two field measurements taken place in both urban and rural areas of East China. The dataset covers a large span of nitric oxide (NO) levels ranging from tens of ppt characteristic of clean rural air to tens of ppb typically found in the polluted urban environment. An observationally constrained zero-dimensional box model that incorporates the CIM mechanism was constructed to simulate the daytime profiles of methacrolein (MACR) and methyl vinyl ketone (MVK), two major first-generation products that account for over half of the total carbon oxidation flow of isoprene. A closer agreement with the measurements was found compared with the traditional mechanism that prescribes a fixed yield of MACR and MVK across all NO levels. This result demonstrates that the isoprene peroxy dynamics operate competitively in the area and play a governing role in the final distribution of isoprene oxidation products. The atmospheric implication is that, with effective measures taken to reduce pollutant emissions in East China, the prevailing chemical regime at play has evolved and implementing the updated isoprene mechanism into regional models will have a profound impact on the predicted radical cycling and ozone production of the local atmosphere.

1. Introduction

Isoprene (2-methyl-1,3-butadiene), the dominant hydrocarbon produced by plants, constitutes nearly half of the carbon flux of nonmethane volatile organic compounds emitted to the atmosphere by the biosphere (Guenther et al., 2012). Once emitted, isoprene is subject to rapid depletion, with an estimated lifetime of around 1 h against oxidation by OH radicals ($\tau_{OH}=1.4$ h for [OH] = 2 × 10⁶ molecules cm⁻³ at T = 298 K), the dominant oxidant in the atmosphere. Owing to such high emission rates and chemical reactivity, the oxidative chemistry of isoprene has a significant influence on the cycling of free radicals and the abundance of ozone and organic aerosols in the troposphere

(Bates and Jacob, 2019; Claeys et al., 2004; Lelieveld et al., 2008; Mao et al., 2013; Paulot et al., 2009; Surratt et al., 2010).

The ambient level of nitric oxide (NO) plays an essential role in the isoprene oxidation cascades by governing the reaction pathways of isoprene peroxy radicals (ISOPOO), a key intermediate produced from the initial attack of OH radicals to the unsaturated carbon chain. In the presence of elevated NO (tens to hundreds of ppbv), the ISOPOO radicals react primarily with NO producing an ensemble of multifunctional oxidation products. This reaction branch has particularly drawn much attention in the past, with a consensus on the branching of two major first-generation products, i.e., ~23% methacrolein (MACR) and ~34% methyl vinyl ketone (MVK)(Galloway et al., 2011; Liu et al., 2013;

^{*} Corresponding author.

^{**} Corresponding author.

E-mail addresses: wanghl@saes.sh.cn (H. Wang), xzhang87@ucmerced.edu (X. Zhang).

¹ Authors contribute equally to this work.

Miyoshi et al., 1994; Paulson and Seinfeld, 1992; Ruppert and Becker, 2000; Sprengnether et al., 2002; Tuazon and Atkinson, 1990). The mechanism developed based on these measurements has been widely incorporated into 3-D transport models to represent the isoprene photochemistry in the urban environment worldwide.

Despite decades of research, isoprene continues to offer surprises to our understanding of its degradation chemistry in the atmosphere. A puzzling question revealed in early 2000s was the unexpectedly high concentrations of OH radicals observed in the forested regions, challenging the earlier mechanism that prescribes a near-complete titration of OH radicals by isoprene (Carslaw et al., 2001; Lelieveld et al., 2008; Martinez et al., 2010). To explain the observed high OH levels, a series of OH recycling mechanisms through the isoprene oxidation cascades have been proposed, among which a notable one is the interconversion of ISOPOO radicals through repetitive O2 addition and dissociation reactions revealed by Peeters et al. (2009 and 2014). This mechanism was later validated by Teng et al. (2017) with observations of isoprene nitrate isomers at a wide range of ISOPOO bimolecular lifetimes, and subsequently compiled in a review by Wennberg et al. (2018). Our recent study further updated this mechanism by monitoring the dynamics of MACR and MVK under precisely controlled chamber conditions (Zhang et al., 2022). This updated mechanism was then validated against a comprehensive dataset of aircraft measurements throughout North America. Here we extend our recent work to diagnose the predominant mechanism that isoprene undergoes in both urban and rural areas of East China, a region with much improved air quality due to effective measures taken to reduce anthropogenic emissions in recent years. With the use of ground-based measurements of an array of trace gases alongside simulations by an observationally constrained zero-dimensional photochemical box model, we demonstrate that the isoprene peroxy interconversion chemistry operates effectively and constantly modulates the isoprene oxidation product distributions in the region.

2. Methods

2.1. Field measurements

The CIIE 2020 (China International Import Expo) field campaign was conducted in the fall of 2020 (Oct. 24 - Nov. 12) on the roof of the research building of the Shanghai Academy of Environmental Sciences located in the urban area of East China (31.170 °N, 121.431°E, 10 m above ground level). The monitoring site is surrounded by commercial and residential sectors and approximately ~300 m away from an expressway to the east. During the campaign, the average temperature, relative humidity, and wind speed were ~291K, ~61%, and ~1.8 m/s, respectively (Peng et al., 2023). The EXPLORE-YRD (EXPeriment on the eLucidation of the atmospheric Oxidation capacity and aerosol foRmation and their Effects in Yangtze River Delta) campaign was carried out in the late spring to early summer of 2018 (May 23 - June 24) at the Jiangsu Provincial Taizhou weather radar station located in Eastern China (32.558 °N, 119.994 °E). This rural site is surrounded by farmlands and approximately 800 m away from two expressways crossing to the southwest. During the campaign, meteorological conditions were relatively warm ($T_{avg} = \sim 295$ K) and humid ($RH_{avg} = \sim 73\%$) with frequent sunshine and low wind speed (WSavg = 2.01 m/s) (Wang et al., 2020).

2.2. Instrumentation

A suite of instruments was used to measure primary gas pollutants including NO_x (Model 42i, Thermo Fischer, USA, DL \sim 60 ppt for Taizhou and DL \sim 0.4 ppb for Shanghai), O_3 (Model 49i, Thermo Fischer, USA), CO (Model 48i, Thermo Fischer, USA), and SO_2 (Model 43C, Thermo Fischer, USA). The photolysis frequencies of O_3 , NO_2 , NO_3 , HONO, HCHO and H_2O_2 were calculated from the spectral actinic flux density

measured by a customized spectral radiometer (Bohn et al., 2008). A custom-built two-channel gas chromatography system equipped with a mass spectrometer and a flame ionization detector (GC-MS/FID) was used to measure over a hundred of non-methane VOCs, including alkanes, alkenes, acetylene, aromatics, halogenated hydrocarbons, and oxygenated VOCs, at hourly time resolution, see the full list of VOCs given in Table 1 in the Supplement. Most C2-C5 hydrocarbons were measured by the FID channel equipped with a PLOT Al₂O₃ column (15 $m \times 0.32$ mm ID, J&W Scientific, USA). Other VOCs were analyzed by the MS channel using a DB-624 column (30 m × 0.25 mm ID, J&W Scientific, USA). Detailed description of the system can be found in Gao et al. (2022). Calibrations were performed on a daily basis with an array of chemical standards comprised of PAMS species (Spectra Gases Inc., USA), U.S. EPA TO-15 calibration mixtures, and a group of OVOCs. Formaldehyde was measured using a commercial Hantzsch monitor (AL4021, Aero-Laser GmbH, Garmisch-Partenkirchen, Germany) with a time resolution of 1 min and a detection limit of 0.02 ppbv, see more details given by Liu et al. (2021).

2.3. Modeling

An observationally constrained 0-D box model was employed to simulate the daytime profiles of MACR and MVK observed during the CIIE 2020 and the EXPLORE-YRD 2018 campaigns. The model was driven by a comprehensive suite of in-situ measurements that characterize the meteorological conditions and the chemical composition of the sampled air masses, including temperature, humidity, pressure, CO, NO_x, O₃, biogenic and anthropogenic VOCs, and photolysis frequencies of O3, NO2, NO3, HONO, HCHO and H2O2. For eight consecutive days during each campaign, the mass balance equation of all compounds constrained in the model read in the instantaneously measured values every hour from local time 08:00 to 18:00. The reaction kinetics and mechanisms for the gas-phase degradation of major VOCs observed during the campaign (including methane, ethane, propane, isobutane, nbutane, isopentane, n-pentane, 2,3-methylpentane, hexane, acetylene, ethylene, isobutene, isoprene, benzene, toluene, m/o/p-xylene, m/o/pethyltoluene, formaldehyde, acetaldehyde, acetone, propanal, n-butanal, acrolein, methyl ethyl ketone, ethanol, propanol, and butanol) were extracted from the Master Chemical Mechanism (MCMv3.3.1, accessible at http://mcm.york.ac.uk). Isoprene reactions kinetics were adopted from the MOZART-TS1 mechanism in the Community Atmosphere Model with Chemistry (CAM-chem) and the Caltech Isoprene Mechanism updated by our recent work (Knote et al., 2014; Lamarque et al., 2012; Wennberg et al., 2018; Zhang et al., 2022). The MOZART-TS1 mechanism represents the traditional understanding of the isoprene photochemistry occurring in two chemical regimes characterized by 'high-NO_x' and 'NO_x-free' conditions. In this mechanism, OH oxidation of isoprene yields two peroxy radicals, one of which further reacts with NO leading to 22.6% MACR and 33.6% MVK, see the detailed list of reactions in Table S2 in the Supplement. The Caltech Isoprene Mechanism includes a series of reactions that describe the repetitive O2 addition and dissociation process between the OH-adducts and ISOPOO radicals, a process that constantly interconverts eight different ISOPOO isomers. The population distribution of each ISOPOO isomer - and their corresponding products — ultimately depend on the dominant ISOPOO removal channel such as bimolecular reactions with NO/HO₂ and H-shift isomerization. As a result, the yield of MACR and MVK (as well as other products) vary with different ISOPOO fates as opposed to a fixed value prescribed in the MOZART-TS1 mechanism. Our recent work has further validated and updated the Caltech Isoprene Mechanism by constraining the ISOPOO interconversion processes with a series of chamber experiments, see the list of reactions given in Table S3 in the Supplement. Such an update has allowed for an accurate representation of the peroxy chemistry in the 1-OH system under moderate-to-high NO_x conditions (Zhang et al., 2022).

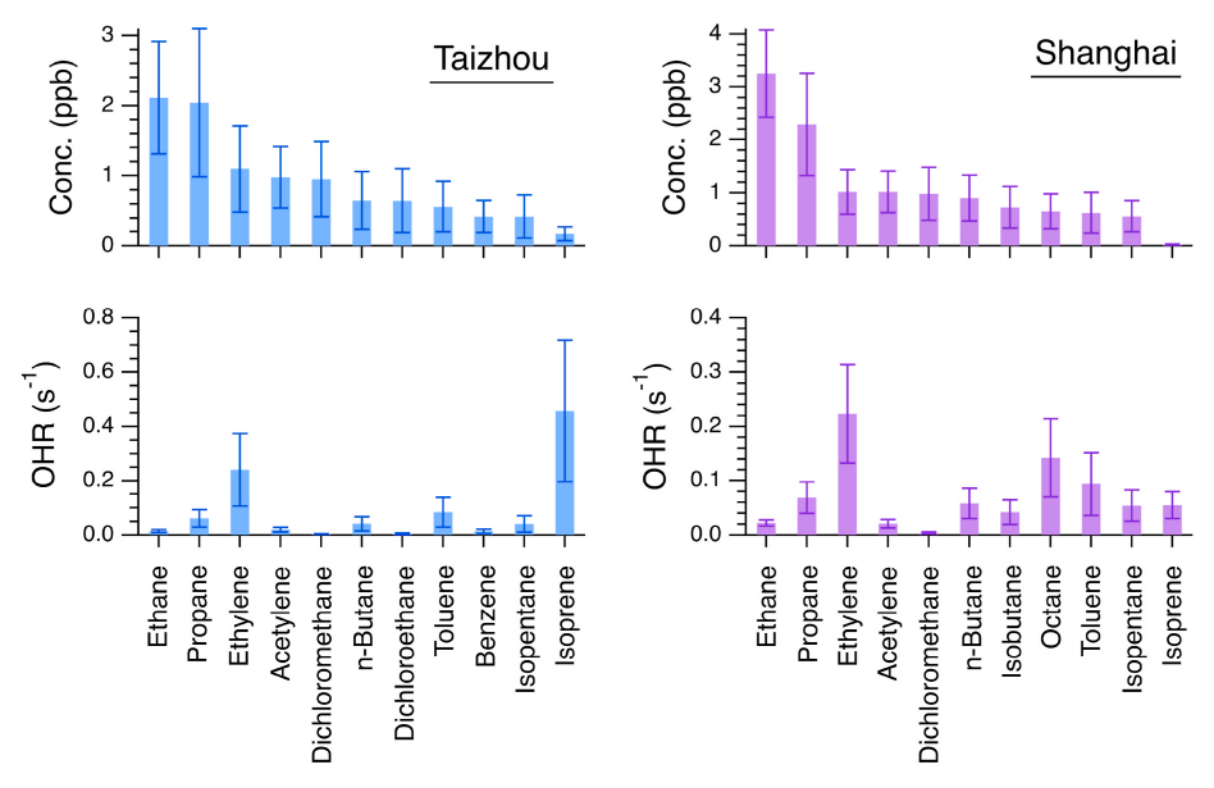


Fig. 1. Average daytime mixing ratios and OH reactivities of isoprene and major anthropogenic NMHCs measured during 10/20/20-11/06/20 in Shanghai (an urban site) and 06/02/18-06/10/18 in Taizhou (a rural site). Error bars represent the standard deviations of the measurements during the periods investigated.

3. Results and discussions

3.1. Contribution of isoprene to the OH reactivity

Average daytime mixing ratios of isoprene at both Shanghai (urban) and Taizhou (rural) sites, together with a group of major non-methane hydrocarbons (NMHCs) of anthropogenic origin, are plotted in Fig. 1. Also shown in Fig. 1 is the corresponding OH reactivity of individual NMHCs, which is calculated based on the rate constant for the reaction of each NMHG with OH radicals (Gao et al., 2022). The abundance of isoprene measured during the late spring season at Taizhou is on the order of hundreds of pptv, which is within the range of the measured isoprene levels in a large number of places in the United States (Baker et al., 2008). The observed level of isoprene is only a small fraction of the major anthropogenic NMHCs emitted, such as small alkanes and aromatic hydrocarbons, which constitute the dominant source of ambient NMHCs at Taizhou. Despite being a relatively small fraction of NMHCs, isoprene contributes to 46.6% of the total OH reactivity against reactions with all NMHCs observed in the area. Emissions of isoprene measured at Shanghai are significantly lower during the late fall season, whereas levels of major anthropogenic NMHCs remain comparable between the two sites. For example, average ethane levels are \sim 2.1 \pm 0.8 ppb at Taizhou vs. 3.3 ± 0.8 ppb at Shanghai. Nevertheless, isoprene still accounts for over ~7% of the OH reactivity out of all thirty-five NMHCs measured (see the full list given in Table S1). Note that the overall OH reactivity at Shanghai during the measurement period was dominated by small OVOCs including formaldehyde and acetaldehyde, which were excluded from the calculation because the photochemistry of isoprene and many other NMHCs constitutes an important source of these small OVOCs. The above analysis reveals that isoprene, the dominant biogenic NMHC, plays an essential role in moderating the oxidation power of the atmosphere even in commonly thought polluted areas such as the Eastern China.

3.2. Spatiotemporal characteristics of methacrolein and methyl vinyl ketone

Here we examine the spatiotemporal characteristics of two major first-generation products from isoprene photooxidation, MACR and MVK, to understand the dynamics of ISOPOO radicals and to identify the prevalent chemical regimes during the two field campaigns. Fig. 2 displays a week-long dataset of isoprene, NO, MACR, and MVK collected from the Shanghai (urban) and Taizhou (rural) sites during the late fall (10/29/2020 - 11/06/2020) and early summer (06/02/2018 - 06/10/2018)2018), respectively. Uncertainties in the measurements are given by $\sqrt{(EF \times Conc)^2 + (DL)^2}$, where EF represents the error fraction or the measurement precision (1.75% for MACR and 1.27% for MVK) and DL is the instrument detection limit (~10 ppt for MACR and ~15 ppt for MVK). Also included are the model predicted daytime (LT 8:00-18:00) profiles of MACR and MVK. Each data point represents the simulated concentration when the production of MACR and MVK from isoprene photooxidation establishes a steady state. A remarkable difference between the two sites is that the observed MACR and MVK appear at much higher levels and with strong diurnal variations at Taizhou, which can be attributed to the intensive biogenic emissions of isoprene in summer combined with sustained ~ ppb levels of NOx throughout the season. Average daytime levels of these two species at Taizhou, i.e., 98.3 ± 72.8 ppt for MACR and 109.2 \pm 77.2 for MVK, are slightly higher than the measurements (MACRavg \sim 36 ppt and MVKavg \sim 60 ppt) taken in the summer of Los Angeles basin (Van Rooy et al., 2021), although the average daytime isoprene concentration is lower by approximately a factor of three at Taizhou. This difference underscores the essential role of NO in regulating the carbon oxidation flows and subsequent product distributions in the isoprene photochemistry because the yields of MACR and MVK depend significantly on the NO level, that is, \sim 24% MACR and ~33% MVK under "high NO" conditions (e.g., >10 ppb NO) vs. ~2% MACR and ~4% MVK under "NO free" conditions (e.g., <10 ppt NO) (Zhang et al., 2022). Compared with the relatively flat temporal profiles

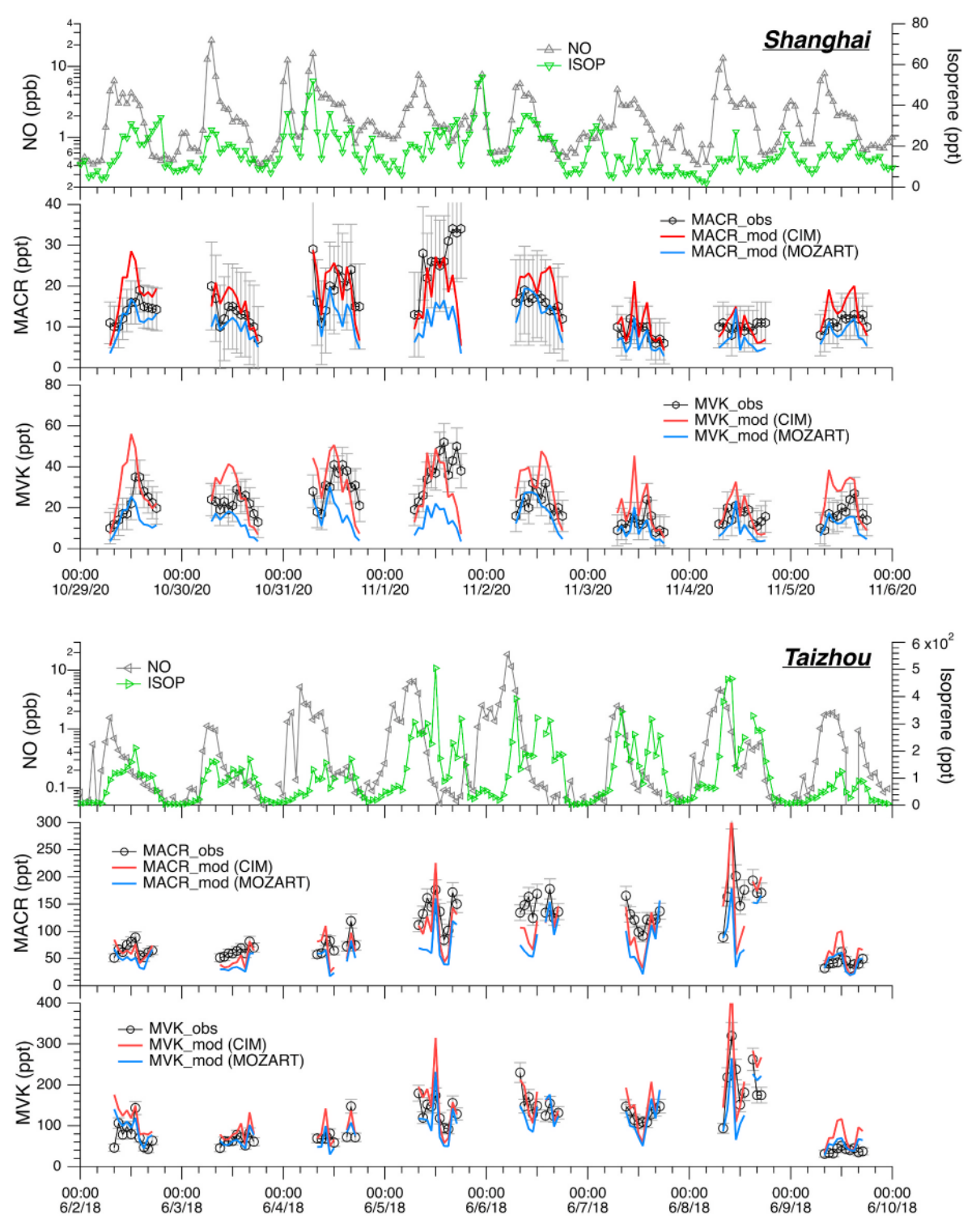


Fig. 2. Observed temporal profiles of isoprene, NO, MACR, and MVK at Shanghai and Taizhou along with model simulations of MACR and MVK with the CIM and MOZART-TS1 mechanisms.

observed at the Shanghai (urban) site in late fall, model simulations, on the other hand, suggest that local MACR and MVK production depends primarily on the solar radiation intensity. Such a difference points to a question: to what degree regional transport affects the composition homogeneity of the observed air masses at the site. As shown in Fig. S1 in the Supplement, the prevailing wind directions alternate between the northwest and the east, and the latter brings air masses from the Pacific Ocean and carries emissions from the harbors along the way, as further

evidenced by the source appointment of $PM_{2.5}$ given in Fig. S2 in the Supplement. The marine air can be enriched by OVOCs including MACR and MVK produced from the photodegradation of dissolved organic matter in seawater (Liss and Johnson, 2014). This likely explains the relatively high background levels of MACR and MVK throughout the observation period, as well as the frequently observed peaks at night that were not captured by the model, as shown in Fig. 2.

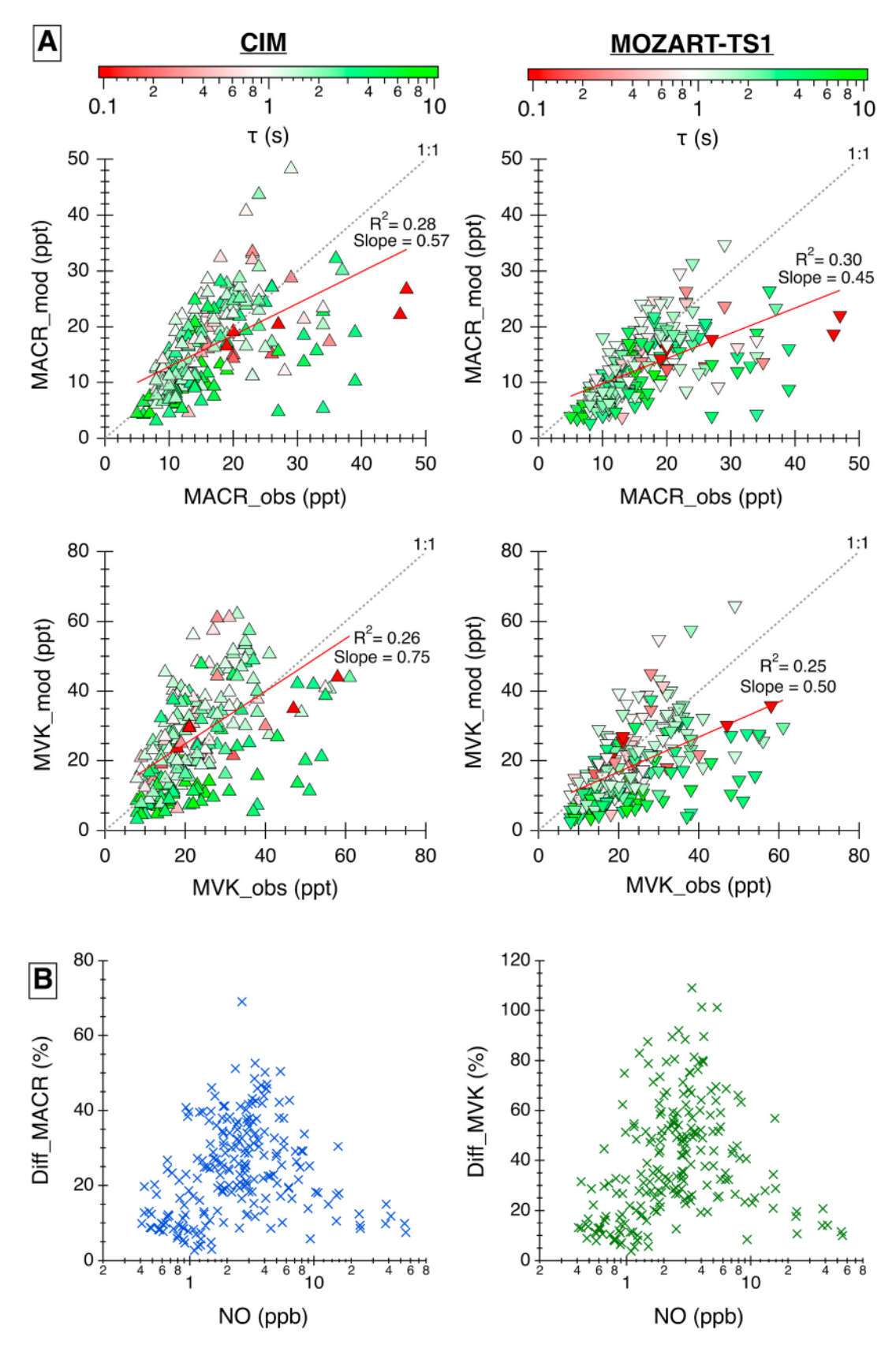


Fig. 3. (A) Scatter plots of the observed daytime mixing ratios of MACR and MVK versus box model simulations using the CIM and MOZART-TS1 mechanism. The dashed black line is the line of equality and the red solid line represents the linear regression on the simulations with the corresponding measurements. (B) Difference in the predictions by the two mechanisms represented by $100\% \times (MACR_{CIM} - MACR_{MOZART})/MACR_{obs}$ and $100\% \times (MVK_{CIM} - MVK_{MOZART})/MVK_{obs}$, respectively.

3.3. Chemical regimes featuring moderate to high NO levels

The EXPLORE-YRD 2018 and CIIE-2020 field campaigns, taken together, cover a broad span of NO levels from a few tens of ppt characteristic of clean rural air to a few tens of ppb typically found in the polluted urban environment. The abundance of NO determines, to a large degree, the bimolecular reactivity of ISOPOO radicals, defined as the ISOPOO bimolecular lifetime with respect to reactions of NO and HO_2 , i.e., $\tau_{RO_2} = 1/(k_{RO_2+NO}[NO]_{ss} + k_{RO_2+HO_2}[HO_2]_{ss})$. Under 'high NO' conditions (e.g., >10 ppb), the dominate fate of ISOPOO radicals is to react with NO and the levels MACR and MVK are determined by the initial kinetic distribution of the six ISOPOO isomers, whereas when NO is limited (e.g., <1 ppb), the ISOPOO radicals may undergo repetitive O2 addition and dissociation processes and the production of MACR and MVK is reflective of a thermal equilibrium distribution of ISOPOO isomers that favors the β-ISOPOO radical, the precursor of MACR and MVK. Our recent chamber results have shown that the production of MACR and MVK at 'low-to-moderate NO' levels can be twice as much as previously found under 'high NO' conditions (Zhang et al., 2022). By examining the extent to which this updated isoprene oxidation mechanism reproduces the observed levels of MACR and MVK at both urban and rural sites of East China, we will develop a comprehensive understanding of the atmospheric relevance of the ISOPOO interconversion chemistry and how this chemistry modulates the final isoprene oxidation product distribution in the area.

Simulated daytime concentrations of MACR and MVK with the updated Caltech Isoprene Mechanism (CIM) and the MOZART-TS1 mechanism incorporated in the box model are compared with the observations given in Fig. 3A. Each data point is color coded by the simulated ISOPOO bimolecular lifetime as an index of the ISOPOO reactivity, that is, the extent to which the interconversion of ISOPOO radicals outcompetes their bimolecular reactions with NO and HO2. The MOZART-TS1 mechanism embedded in the CAM-chem global model is considered a classic representation of the isoprene photooxidation pathway in the presence of NOx, see details in the Methods section. The updated CIM describes explicitly the interactions between the ISOPOO isomers and the hydroxy allylic radicals using eight O2 addition and dissociation reactions, see Table S2 in the Supplement. Model outputs with the MOZART-TS1 mechanism in general underpredict MACR and MVK, with the normalized mean biases (NMB) of -22.5% and -21.48%, respectively. Simulations with the updated CIM mechanism are in closer agreement with the measurements (NMB $\sim -1.24\%$ for MACR and 13.45% for MVK). More statistical evaluation indexes for the performance of these two mechanisms are provided in Table S4 in the Supplement. The disagreement between the two mechanisms becomes evident when the NO level falls within the 1-10 ppb range (Fig. 3B), which is expected because the ISOPOO interconversion becomes competitive or even dominates over their bimolecular reactions with NO, leading to elevated β-ISOPOO radicals and thus promoting the formation MACR and MVK. The closer agreement between measurements from the two sites and simulations with the CIM mechanism provides direct evidence that the isoprene peroxy interconversion process operates effectively in both urban and rural areas typically found in East China. This signifies that the prevalent chemical regime in the area is no longer the "high NOx" conditions thought previously.

4. Conclusions

We validated the recently updated isoprene photooxidation mechanism (CIM) using two comprehensive datasets collected from the EXPLORE-YRD-2018 and the CIIE-2020 field campaigns carried out in regions of East China. These two campaigns, taken place in Shanghai (the most populous urban area in China) and Taizhou (a rural area with an agriculture-based economy), cover a broad range atmospheric photochemical conditions characterized by tens of ppt to tens of ppb levels of NO. A 0-D box model that accounts for the complex interplay of

meteorological variations and atmospheric oxidative processes was developed with two independent mechanisms incorporated, i.e., the updated CIM and the MOZART-TS1. The comparison of model simulations with measurements allows for the assessment of the extent to which the updated CIM mechanism is representative of the actual atmospheric conditions in the area. We show that the model with the updated CIM mechanism adequately captures the diurnal variations of MACR (NMB~-1.24%) and MVK (NMB~13.45%), two major firstgeneration products that account for up to ~76% of the total carbon oxidation flow of isoprene across all NO levels investigated. Such an agreement suggests that the ISOPOO radical, a key intermediate produced from the initial OH attack to the isoprene backbone, undergoes interconversions through O2 addition and dissociation in addition to the bimolecular reactions with NO/HO_2 as their exclusive fate thought previously. The direct consequence of the changing behaviors of ISO-POO radicals is to alter the isoprene final oxidation product distributions. As the photooxidation of MACR contributes primarily to the formation secondary organic aerosols (SOA) under "moderate-to-high NO_x" conditions in the isoprene system (Nguyen et al., 2015), the changing product distribution will affect the overall SOA budget produced from the isoprene photochemistry in the area. Moreover, the interconversion and subsequent isomerization of ISOPOO radicals provide pathways for the cycling and regeneration of HOx radicals, thereby affecting the overall O3 accumulation at given NOx levels (Wennberg et al., 2018). With series of effective measures taken by the Chinese government to reduce anthropogenic emissions including NOx (Zhu et al., 2023), how the isoprene photochemistry plays a role in modulating the chemical composition and the oxidation capacity of the regional atmosphere needs to be reassessed.

Declaration of competing interest

The authors declare that they have no known competing financial interests or personal relationships that could have appeared to influence the work reported in this paper.

Data availability

Data will be made available on request.

Acknowledgements

This work is supported by the U.S. National Science Foundation Grant AGS-2131199.

Appendix A. Supplementary data

Supplementary data to this article can be found online at https://doi.org/10.1016/j.apgeochem.2023.105778.

References

Baker, A.K., Beyersdorf, A.J., Doezema, L.A., Katzenstein, A., Meinardi, S., Simpson, I.J., Blake, D.R., Rowland, F.S., 2008. Measurements of nonmethane hydrocarbons in 28 United States cities. Atmos. Environ. 42, 170–182.

Bates, K.H., Jacob, D.J., 2019. A new model mechanism for atmospheric oxidation of isoprene: global effects on oxidants, nitrogen oxides, organic products, and secondary organic aerosol. Atmos. Chem. Phys. 19, 9613–9640.

Bohn, B., Corlett, G.K., Gillmann, M., Sanghavi, S., Stange, G., Tensing, E., Vrekoussis, M., Bloss, W., Clapp, L., Kortner, M., 2008. Photolysis frequency measurement techniques: results of a comparison within the ACCENT project. Atmos. Chem. Phys. 8, 5373–5391.

Carslaw, N., Creasey, D., Harrison, D., Heard, D., Hunter, M., Jacobs, P., Jenkin, M., Lee, J., Lewis, A., Pilling, M., 2001. OH and HO2 radical chemistry in a forested region of north-western Greece. Atmos. Environ. 35, 4725–4737.

Claeys, M., Graham, B., Vas, G., Wang, W., Vermeylen, R., Pashynska, V., Cafmeyer, J., Guyon, P., Andreae, M.O., Artaxo, P., 2004. Formation of secondary organic aerosols through photooxidation of isoprene. Science 303, 1173–1176.

Galloway, M., Huisman, A., Yee, L., Chan, A., Loza, C., Seinfeld, J., Keutsch, F., 2011.
Yields of oxidized volatile organic compounds during the OH radical initiated

- oxidation of isoprene, methyl vinyl ketone, and methacrolein under high-NO x conditions. Atmos. Chem. Phys. 11, 10779–10790.
- Gao, Y., Wang, H., Liu, Y., Zhang, X., Jing, S., Peng, Y., Huang, D., Li, X., Chen, S., Lou, S., 2022. Unexpected high contribution of residential biomass burning to nonmethane organic gases (NMOGs) in the Yangtze River Delta region of China. J. Geophys. Res. Atmos. 127, e2021JD035050.
- Guenther, A., Jiang, X., Heald, C.L., Sakulyanontvittaya, T., Duhl, T.a., Emmons, L., Wang, X., 2012. The Model of Emissions of Gases and Aerosols from Nature version 2.1 (MEGAN2. 1): an extended and updated framework for modeling biogenic emissions. Geosci. Model Dev. (GMD) 5, 1471–1492.
- Knote, C., Hodzic, A., Jimenez, J., Volkamer, R., Orlando, J., Baidar, S., Brioude, J., Fast, J., Gentner, D., Goldstein, A., 2014. Simulation of semi-explicit mechanisms of SOA formation from glyoxal in aerosol in a 3-D model. Atmos. Chem. Phys. 14, 6213–6239.
- Lamarque, J.-F., Emmons, L., Hess, P., Kinnison, D.E., Tilmes, S., Vitt, F., Heald, C., Holland, E.A., Lauritzen, P., Neu, J., 2012. CAM-Chem: description and evaluation of interactive atmospheric chemistry in the community earth system model. Geosci. Model Dev. (GMD) 5, 369–411.
- Lelieveld, J., Butler, T., Crowley, J., Dillon, T., Fischer, H., Ganzeveld, L., Harder, H., Lawrence, M., Martinez, M., Taraborrelli, D., 2008. Atmospheric oxidation capacity sustained by a tropical forest. Nature 452, 737–740.
- Liss, P.S., Johnson, M.T., 2014. Ocean-atmosphere Interactions of Gases and Particles. Springer Nature.
- Liu, Y., Herdlinger-Blatt, I., McKinney, K., Martin, S., 2013. Production of methyl vinyl ketone and methacrolein via the hydroperoxyl pathway of isoprene oxidation. Atmos. Chem. Phys. 13, 5715–5730.
- Liu, Y., Wang, H., Jing, S., Peng, Y., Gao, Y., Yan, R., Wang, Q., Lou, S., Cheng, T., Huang, C., 2021. Strong regional transport of volatile organic compounds (VOCs) during wintertime in Shanghai megacity of China. Atmos. Environ. 244, 117940.
- Mao, J., Paulot, F., Jacob, D.J., Cohen, R.C., Crounse, J.D., Wennberg, P.O., Keller, C.A., Hudman, R.C., Barkley, M.P., Horowitz, L.W., 2013. Ozone and organic nitrates over the eastern United States: sensitivity to isoprene chemistry. J. Geophys. Res. Atmos. 118 (11), 256, 211,268.
- Martinez, M., Harder, H., Kubistin, D., Rudolf, M., Bozem, H., Eerdekens, G., Fischer, H., Klüpfel, T., Gurk, C., Königstedt, R., 2010. Hydroxyl radicals in the tropical troposphere over the Suriname rainforest: airborne measurements. Atmos. Chem. Phys. 10, 3759–3773.
- Miyoshi, A., Hatakeyama, S., Washida, N., 1994. OH radical-initiated photooxidation of isoprene: an estimate of global CO production. J. Geophys. Res. Atmos. 99, 18779–18787.
- Nguyen, T.B., Bates, K.H., Crounse, J.D., Schwantes, R.H., Zhang, X., Kjaergaard, H.G., Surratt, J.D., Lin, P., Laskin, A., Seinfeld, J.H., 2015. Mechanism of the hydroxyl radical oxidation of methacryloyl peroxynitrate (MPAN) and its pathway toward secondary organic aerosol formation in the atmosphere. Phys. Chem. Chem. Phys. 17, 17914-17926.

- Paulot, F., Crounse, J.D., Kjaergaard, H.G., Kürten, A., St Clair, J.M., Seinfeld, J.H., Wennberg, P.O., 2009. Unexpected epoxide formation in the gas-phase photooxidation of isoprene. Science 325, 730-733.
- Paulson, S.E., Seinfeld, J.H., 1992. Development and evaluation of a photooxidation mechanism for isoprene. J. Geophys. Res. Atmos. 97, 20703–20715.
- Peeters, J., Muller, J.-F.o., Stavrakou, T., Nguyen, V.S., 2014. Hydroxyl radical recycling in isoprene oxidation driven by hydrogen bonding and hydrogen tunneling: the upgraded LIM1 mechanism. J. Phys. Chem. 118, 8625–8643.
- Peeters, J., Nguyen, T.L., Vereecken, L., 2009. HO x radical regeneration in the oxidation of isoprene. Phys. Chem. Chem. Phys. 11, 5935–5939.
- Peng, Y., Wang, H., Gao, Y., Jing, S., Zhu, S., Huang, D., Hao, P., Lou, S., Cheng, T., Huang, C., 2023. Real-time measurement of phase partitioning of organic compounds using a proton-transfer-reaction time-of-flight mass spectrometer coupled to a CHARON inlet. Atmos. Meas. Tech. 16, 15–28.
- Ruppert, L., Becker, K.H., 2000. A product study of the OH radical-initiated oxidation of isoprene: formation of C5-unsaturated diols. Atmos. Environ. 34, 1529–1542.
- Sprengnether, M., Demerjian, K.L., Donahue, N.M., Anderson, J.G., 2002. Product analysis of the OH oxidation of isoprene and 1, 3-butadiene in the presence of NO. J. Geophys. Res. Atmos. 107. ACH 8-1-ACH 8-13.
- Surratt, J.D., Chan, A.W., Eddingsaas, N.C., Chan, M., Loza, C.L., Kwan, A.J., Hersey, S. P., Flagan, R.C., Wennberg, P.O., Seinfeld, J.H., 2010. Reactive intermediates revealed in secondary organic aerosol formation from isoprene. Proc. Natl. Acad. Sci. USA 107. 6640-6645.
- Teng, A.P., Crounse, J.D., Wennberg, P.O., 2017. Isoprene peroxy radical dynamics. J. Am. Chem. Soc. 139, 5367–5377.
- Tuazon, E.C., Atkinson, R., 1990. A product study of the gas-phase reaction of isoprene with the OH radical in the presence of NOx. Int. J. Chem. Kinet. 22, 1221–1236.
- Van Rooy, P., Tasnia, A., Barletta, B., Buenconsejo, R., Crounse, J.D., Kenseth, C.M., Meinardi, S., Murphy, S., Parker, H., Schulze, B., 2021. Observations of volatile organic compounds in the Los Angeles basin during COVID-19. ACS Earth Space Chem. 5, 3045–3055.
- Wang, H., Gao, Y., Wang, S., Wu, X., Liu, Y., Li, X., Huang, D., Lou, S., Wu, Z., Guo, S., 2020. Atmospheric processing of nitrophenols and nitrocresols from biomass burning emissions. J. Geophys. Res. Atmos. 125, e2020JD033401.
- Wennberg, P.O., Bates, K.H., Crounse, J.D., Dodson, L.G., McVay, R.G., Mertens, L.A., Nguyen, T.B., Praske, E., Schwantes, R.H., Smarte, M.D., 2018. Gas-phase reactions of isoprene and its major oxidation products. Chem. Rev. 118, 3337–3390.
- Zhang, X., Wang, S., Apel, E.C., Schwantes, R.H., Hornbrook, R.S., Hills, A.J., DeMarsh, K.E., Moo, Z., Ortega, J., Brune, W.H., 2022. Probing isoprene photochemistry at atmospherically relevant nitric oxide levels. Chem 8, 3225–3240.
- Zhu, T., Tang, M., Gao, M., Bi, X., Cao, J., Che, H., Chen, J., Ding, A., Fu, P., Gao, J., 2023. Recent progress in atmospheric chemistry research in China: establishing a theoretical framework for the "air pollution complex". Adv. Atmos. Sci. 1–23.